

## ChemComm

## Dynamic Covalent and Noncovalent Assembly of o-Nitrosocumene in Organic Solvents and Water

Journal:	ChemComm
Manuscript ID	CC-COM-08-2024-003955.R1
Article Type:	Communication

SCHOLARONE™ Manuscripts

### ChemComm

## COMMUNICATION

# Dynamic Covalent and Noncovalent Assembly of *o*-Nitrosocumene in Organic Solvents and Water

Received 00th January 20xx, Accepted 00th January 20xx

DOI: 10.1039/x0xx000000x

Cory H. Rogers,<sup>a</sup> Anu Pradeep,<sup>b</sup> Layla A. Galiano,<sup>a</sup> S. Ariel Kelley,<sup>a</sup> Ramkumar Varadharajan,<sup>b</sup> Ken Belmore,<sup>a</sup> Logan M. Whitt,<sup>a</sup> Yanmei Li,<sup>c</sup> Pier Alexandre Champagne,<sup>c</sup> Vaidhyanathan Ramamurthy,\*<sup>b</sup> Silas C. Blackstock\*<sup>a</sup>

Ortho-nitrosocumene (o-NC) exhibits dynamic N,N bonding, interchanging monomer and E/Z-azodioxide dimer structures, the extent of which depends on environment. As a solid, o-NC is a Z-dimer; in organic solvent, monomer is favored; and in water, dimers are favored. A supramolecular assembly of o-NC is observed as a separate species by NMR in water, shown to be a novel nanometer-sized aggregate containing ~2000 molecules.

Assembly of molecules into structured domains enables the formation and function of molecular systems. Dynamic covalent bonding (DCB) offers a unique modality for temporal, yet rigid molecular assembly, with linkage strengths between 'loose' noncovalent attractions and the 'tight' covalent bonds of stable molecules.¹ DCB finds application in smart materials such as self-healing and shape-memory polymers.² Nitrosobenzenes undergo DCB to reversibly form E- and Z-azodioxides.³,4 Our recent study of *p*-nitrosocumene evaluated its assembly properties in water as influenced by organic hosts.⁵ For isomeric *o*-nitrosocumene (*o*-NC), the focus of this report, the *nature* of its DCB assembly (Scheme 1) is found to be strongly medium dependent (even in the absence of hosts) and a new noncovalent 'NMR-active' nanoassembly is discovered in water.

Scheme 1 o-NC dynamic N,N covalent bonding

 $\emph{o}\text{-NC}$  was prepared by oxone  $^{TM}$  oxygenation of  $\emph{o}\text{-}$  aminocumene in biphasic H2O/CH2Cl2. Green CH2Cl2 solutions

of monomeric o-NC, upon cooling, afford colorless crystals of the Z-azodioxide dimer,  $D_Z(anti)$ , whose structure was determined by X-ray diffraction (Fig. 1). This dimer has an N,N bond length of 1.32 Å with ONNO angle of 1.9° and contains phenyl rings twisted  $^{\sim}71^{\circ}$  out of the azodioxide plane with *anti i*-Pr groups geared to the phenyl ring planes.

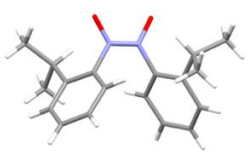


Fig. 1 X-ray structure of o-NC dimer crystal, D<sub>z</sub>(anti)

Upon dissolution in organic solvents, colorless o-NC crystals yield green solutions containing mostly monomeric (M) o-NC. At high concentrations (typically > 0.1 M) and low temperatures (<25 to -70 °C), E/Z-azodioxide dimers (D) form and are observable by <sup>1</sup>H-NMR spectroscopy. The M,D interconversion is slow on the NMR timescale, yielding distinct, sharp <sup>1</sup>H-NMR signals for M and D species, which remain fully equilibrated at > -50 °C. Figure 2 shows the o-NC <sup>1</sup>H-NMR spectrum at 31 °C in CD<sub>3</sub>OD and upon cooling to -71 °C. The warmer solution contains almost entirely o-NC monomer (red M labels) while in the colder solution o-NC dimers (blue and green highlights) predominate. Warming the cold solution regenerates the Mrich composition. To assign the o-NC D<sub>z</sub> dimer NMR signals, o-NC D<sub>Z</sub> crystals were dissolved in CD<sub>3</sub>OD at -68 °C to give a colorless solution, yielding only the blue-highlighted signals of Fig. 2 (Fig. S10). The remaining minor set of o-NC dimer signals (green highlights, Fig. 2B) are assigned to the D<sub>F</sub> dimer. At low temperature, the D<sub>Z</sub> population of o-NC predominates over the D<sub>E</sub> and M forms, with M predominating at ambient.

Noteworthy features of the Fig. 2 spectra include: (a) highly shielded  $H_a$  and highly deshielded  $H_e$  signals in M due to the strong shielding cone of the oriented nitroso group, <sup>7b,8</sup> and (b) distinct  $D_Z$  NMR signals for diastereotopic *i*-Pr methyl groups at low temperature due to hindered N-phenyl rotation.<sup>9</sup>

a. Department of Chemistry and Biochemistry, The University of Alabama, Tuscaloosa, AL 35487, USA. E-mail: blackstock@ua.edu

b. Department of Chemistry, University of Miami, Coral Gables, FL 33124, USA

<sup>&</sup>lt;sup>c</sup> Department of Chemistry and Environmental Science, New Jersey Institute of Technology, Newark, NJ 07102, USA

<sup>†</sup> Electronic supplementary information (ESI) available. CCDC 2313924, <a href="https://www.ccdc.cam.ac.uk/data\_request/cif">www.ccdc.cam.ac.uk/data\_request/cif</a>. See DOI: 10.1039/x0xx00000x

COMMUNICATION ChemComm

EXSY (exchange spectroscopy)  $NMR^{10}$  is employed to probe the M,  $D_Z$ ,  $D_E$  interconversion pathways in  $CDCl_3$  and assign the  $^1H$ -NMR signals of  $D_Z$  and  $D_E$  (Figs. S11-S13). Chemical exchange is observed for M, $D_Z$  and M, $D_E$  but not between  $D_Z$ , $D_E$ , indicating that the covalently linked dimers interconvert only by dissociation/reassembly and not by N,N bond rotation, as also found for the parent nitrosobenzene.  $^{11}$  DFT calculations  $^{12}$  of N,N cleavage barriers give  $\Delta G^z = 94$  kJ/mol and  $^{11}$ 0 kJ/mol for  $D_Z$  to 2M and  $D_E$  to 2M dissociations, respectively (Fig. S36).

Given the different dipole moments of the o-NC forms (computed $^{11}$  as M 4.60, D<sub>Z</sub> 8.69, and D<sub>E</sub> 0.10 debye), a solvent polarity effect on the extent of N,N bond formation might be expected. Knowing the M, D<sub>Z</sub>, and D<sub>E</sub>  $^{1}$ H-NMR signal assignments, we have examined the medium effect on the degree of D assembly for o-NC. VT-NMR experiments in CDCl<sub>3</sub>, (CD<sub>3</sub>)<sub>2</sub>CO, CD<sub>3</sub>OD, CD<sub>3</sub>CN and D<sub>2</sub>O were conducted, and results for the D-to-2M (monomerization) interchange are given in Table 1. An internal standard (mesitylene or dimethylsulfone) was used to quantitate concentrations and an internal CD<sub>3</sub>OD capillary $^{13}$  was used to monitor sample temperature.

As noted in Table 1, solution phase N,N bond dissociation energies (BDEs) of 36-55 kJ/mol (8.6-13 kcal/mol) are observed for the azodioxides. These weak solution BDEs are the basis for nitrosobenzene N,N dynamic covalent bonding. N,N bond formation is counter-balanced by -TΔS factors favoring N,N cleavage to monomer such that M, D<sub>Z</sub> and D<sub>E</sub> forms of o-NC are all populated at readily attainable concentrations and temperatures. The data for o-NC in  $\text{CDCl}_3$  are similar in magnitude to that of nitrosobenzene<sup>11,14</sup> in CDCl<sub>3</sub>, which has  $\Delta H^{\circ} = 55.5$ , 42.5 kJ/mol,  $\Delta S^{\circ} = 219$ , 185 J/K mol, and  $\Delta G^{\circ} = -9.8$ , -12.5 kJ/mol for  $D_Z$  and  $D_E$  monomerization, respectively. In organic solvents at 298 K, monomeric o-NC is favored. Less polar organic solvents (CDCl3, (CD3)2CO) favor M ( $\Delta G^{\circ}$  -7.1 – -9.0 kJ/mol) more than polar organic solvents (CD<sub>3</sub>OD, CD<sub>3</sub>CN) (ΔG° -2.3 – -4.5 kJ/mol). A large change is observed in water, favoring D formation ( $\Delta G^{\circ}$  14.3 – 17.4 kJ/mol) even at mM concentrations, 1000 x lower than required for D assembly in CDCl<sub>3</sub>.

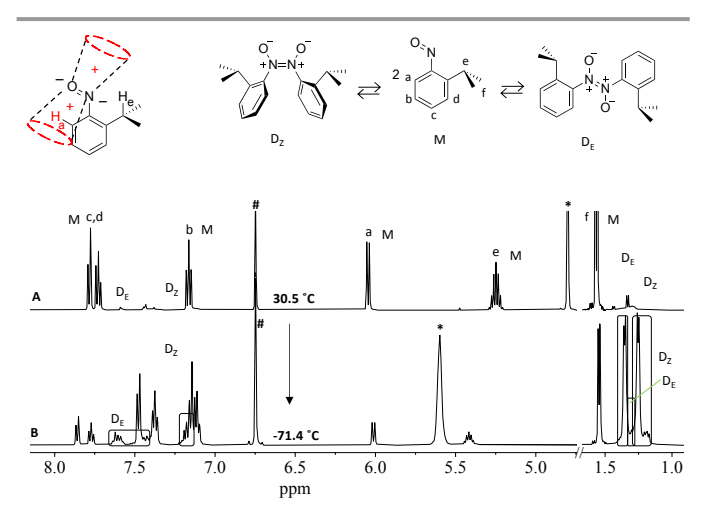


Fig. 2  $^{\circ}$ H-NMR spectrum (500 MHz, 0.130 M in CD $_{3}$ OD) of o-NC at (A) 30.5  $^{\circ}$ C (mostly M (red)), (B) -71.4  $^{\circ}$ C (mostly D $_{z}$  (blue)) \* CD $_{3}$ OH residual solvent, # mesitylene internal standard.

Table 1 o-NC D-to-2M conversions solvent effect by VT-NMR analysis<sup>a</sup>

Solvent (ε) <sup>b</sup>	[total o-NC]		ΔH* (kJ/mol)	ΔS° (J/mol*K)	ΔG* 298 K (kJ/mol)	K <sub>m</sub> 298 K (M)	ΔT (°C)
CDCI <sub>3</sub> (4.8)	0.363 M	Dz	54.8 ± 1.9	209 ± 7	-7.4 ± 0.3	20 ± 2	-44.8 - 35.2
		D <sub>E</sub>	41.2 ± 0.8	162 ± 3	-7.1 ± 0.1	18 ± 1	
(CD <sub>3</sub> ) <sub>2</sub> CO (20)	0.275 M	Dz	48.8 ± 0.8	194 ± 3	-9.0 ± 0.1	38 ± 2	-55.9 – 30.3
		D <sub>E</sub>	38.6 ± 0.8	153 ± 3	-7.1 ± 0.1	18 ± 1	
CD <sub>3</sub> OD (33)	0.190 M	Dz	45.3 ± 1.1	160 ± 4	-2.3 ± 0.1	2.6 ± 0.1	-47.2 - 29.6
		D <sub>E</sub>	35.3 ± 0.5	133 ± 2	-4.3 ± 0.1	5.6 ± 0.1	
CD <sub>3</sub> CN (38)	0.109 M	Dz	49.1 ± 0.3	180 ± 1	-4.5 ± 0.2	6.1 ± 0.4	-39.4 28.1
		DE	39.7 ± 1.1	147 ± 4	-4.1 ± 0.1	5.2 ± 0.1	
D <sub>2</sub> O (80)	0.546 mM	D <sub>z</sub>	54.4 ± 1.7	124 ± 6	17.4 ± 0.1	0.00088 ± 0.00003	3.3 – 37.2
		Dį	39.3 ± 1.6	84 ± 5	14.3 ± 0.1	0.0032 ± 0.0001	
A in D <sub>2</sub> O <sup>c</sup>	21.4 M	D <sub>2</sub>	20	141	-12.2	137	- 25
		DE	58	55.	-12.2	137	

(a)  $R^2 > 0.99$  for all Van't Hoff linear regressions, (b) solvent dielectric constant at 25 °C (c) aggregate in  $D_2O$ 

The driving force for D assembly of o-NC in water is thought to arise from specific H-bonded stabilization of the azodioxide structures in water, in combination with the hydrophobic effect,  $^{15}$  the latter indicated by a lower  $\Delta S^{\circ}$  in  $D_2O$  than in organic solvent (Table 1). DFT calculations also predict dimer preference in water compared to M preference in chloroform (Figs. S34 and S36). In support of preferential H-bonded solvation of D structures by water, the computed  $\Delta G^{\circ}$  for 2M dimerization to  $D_z$  is 7.9 kJ/mol more exergonic when two explicit water molecules hydrogen-bonded to the oxygen atoms are included (Fig. S40).

As o-NC concentration in  $D_2O$  is increased above ~1 mM, a new set of  ${}^1H$ -NMR signals appear, which eventually become the major component of the spectrum as shown in Fig. 3 (violet highlights).  ${}^{16}$  These new signals are sharp, appear in a constant ratio, and are more shielded than the o-NC M and D signals in water. Additionally, we notice that the solution becomes turbid with increasing additions of o-NC. The newly emerging NMR signals in water appear to be *new forms* of o-NC and are observed only in aqueous medium. We propose that an 'NMR aggregate' forms in water (see Scheme 2, violet highlight). The NMR aggregate retains its own sharp, discrete NMR signals.

Of particular note, the methyl region of the spectrum shows a 4:1:1 d:d:br-s set of signals ascribed to aggregate i-Pr methyl groups. Most diagnostic of the aggregate signals is the doublet at 5.5 ppm, which must belong to a new form of o-NC monomer, based on its chemical shift (i.e. within -NO shielding cone). By integration, the starred signals of Fig. 3C can thus be assigned to a 'new', more shielded o-NC monomer. The smaller signals at 0.75-1.0 ppm are presumed to be methyl i-Pr groups of E/Z-azodioxides, also in a new, more shielded environment. Scheme 2 depicts the full o-NC assembly process, including the NMR aggregate phase of M,  $D_z$ , and  $D_E$  (designated  $A_M$ ,  $A_z$ , and  $A_E$ ).  $^{17}$ 

EXSY-NMR analysis of the  $D_2O$  sample confirms the exchange of the proposed aggregate phase components ( $A_M$ ,  $A_Z$ ,

Journal Name COMMUNICATION

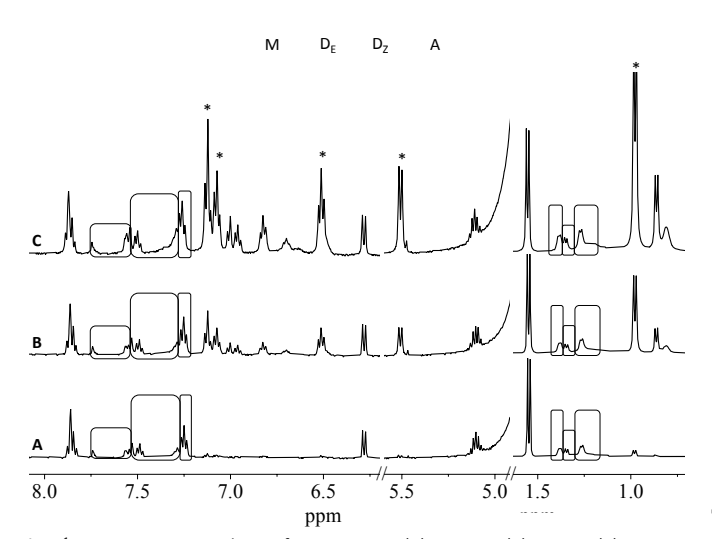


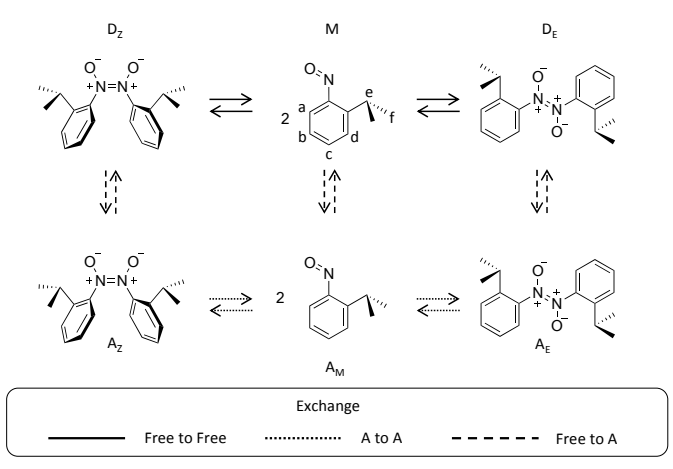
Fig. 3  $^1$ H-NMR spectra at ambient of o-NC in  $D_2O$  at (A) 0.75 mM, (B) 1.5 mM, (C) 3.0 mM.

 $A_E$ ) with 'free' M,  $D_Z$ , and  $D_E$  structures, respectively. Fig. 4 shows EXSY-NMR correlations for the methyl signals of the  $D_2O$  sample. The aggregate i-Pr methyl signals exchange with the free M,  $D_Z$ , and  $D_E$  i-Pr signals, confirming their assignments (dashed lines of Fig. 4). Likewise, the other proton resonances of free M exchange with the corresponding  $A_M$  signals (Figs. S30-S31), and the same is observed for  $D_Z/A_Z$  and  $D_E/A_E$  signal exchanges, confirming these interconversions and yielding the signal assignments. Exchange due to dynamic covalent N,N bonding within the aggregate phase components ( $A_M/A_Z$  and  $A_M/A_E$  dotted lines of Fig. 4) is also observed. <sup>18</sup>

As the amount of o-NC (as stock solution in DMSO-d<sub>6</sub>) is increased incrementally beyond 1 mM, more NMR active aggregate is observed (Fig. 3). Quantitation by NMR signal integration relative to a  $\text{Me}_2\text{SO}_2$  internal standard shows that the dissolved M and D signals remain steady at their saturation values, while the aggregate signals grow in intensity. The solution also grows more turbid and not all the added o-NC is being observed in the NMR spectrum (Fig. S26).<sup>19</sup>

DOSY NMR analysis<sup>20</sup> (Fig. S33) provides diffusion constants and related hydrodynamic radii of the M, D, and A components in D<sub>2</sub>O (Table 2). DOSY radii of M and D are 2.5 and 3.5 Å, respectively, at the expected order of magnitude. The A component signals all show the same larger radii of ~ 33 Å, consistent with a single dynamic ensemble of  $A_{\text{M}}$ ,  $A_{\text{Z}}$ , and  $A_{\text{E}}$  in the NMR aggregate. Interestingly, time incremental DOSY measurements show that, after an initial 'relaxation' period, the aggregate 'droplet' size remains roughly constant for hours, with a radius of ~3 nm and a composition of  $M_8D_zD_E$ . This stoichiometric ratio of aggregate components remains constant regardless of the total amount of NMR aggregate present in solution, as expected for an equilibrated o-NC phase. While persistent in size, the NMR active aggregate is metastable, and its NMR signal diminishes over hours as a bulk phase separation (droplet coalescence) slowly occurs (Fig. S28).

Using the DOSY-derived M, D, and A sizes, the NMR active aggregate of o-NC in  $D_2O$  is estimated to contain  $\sim 2000$  molecules. <sup>21</sup> This aggregate phase is hydrophobic and gives rise



Scheme 2 Proposed o-NC assemblies in D<sub>2</sub>O (violet shading is 'NMR' aggregate phase)

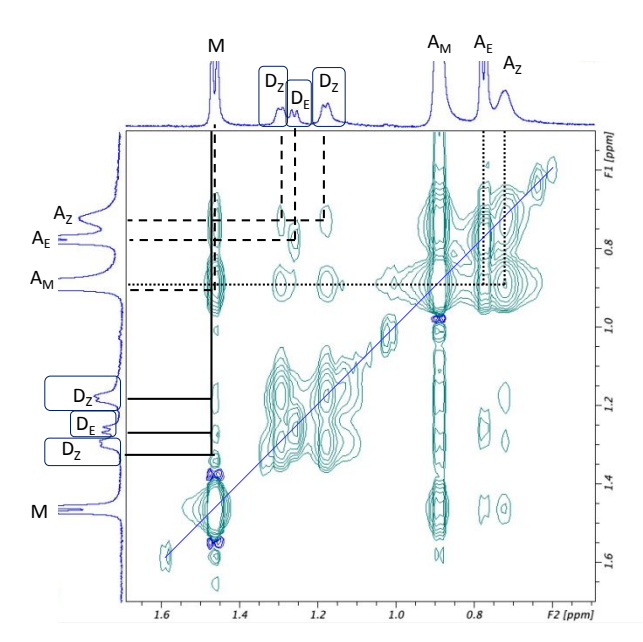


Fig. 4 2D EXSY NMR spectrum ( $D_2O$ , 500 MHz) of 2.40 mM  $\sigma$ -NC, methyl region. Depicted is (as in Scheme 2) chemical exchange between free M and D in solution (solid lines), between M and D within aggregate phase (dotted lines), and between free M,D with aggregate M,D (dashed lines) (see S30-S32 for full EXSY spectra).

to ~0.5 ppm shielding of its component NMR signals, compared to o-NC structures dissolved in D<sub>2</sub>O. The equilibrium constant K for monomerization within the aggregate is ~137 M (Table 1), 160,000 x that in D<sub>2</sub>O ( $\Delta\Delta G^{\circ}$  ~ 29.8 kJ/mol).

 $\textbf{Table 2} \ \mathsf{DOSY} \ \mathsf{diffusion} \ \mathsf{coefficients} \ \mathsf{and} \ \mathsf{hydrodynamic} \ \mathsf{radii} \ \mathsf{of} \ \mathsf{M,D,} \ \mathsf{and} \ \mathsf{A} \ \mathsf{forms} \ \mathsf{of} \ \textit{o-}\mathsf{NC}$ 

	Monomer		Dir	ner	Aggregate	
Time (hrs)	Da	R <sup>b</sup>	Da	R <sup>b</sup>	D <sup>a</sup>	R <sup>b</sup>
3.2	9.67	2.54	6.34	3.87	0.624	39.3
7.5	10.3	2.39	7.59	3.23	0.717	34.2
12	10.2	2.42	7.35	3.34	0.733	33.4
15	9.92	2.47	6.70	3.66	0.743	33.0
23	10.1	2.43	7.14	3.44	0.820	29.9

(a) D = Diffusion coefficient ( $10^{10}$  m $^2$ /s), (b) R = hydrodynamic radius (Å) from Stokes-Einstein Eq.

COMMUNICATION ChemComm

In summary, we find a strong medium effect on the degree and nature of o-NC assembly. Monomer is favored in organic solvent and N,N-bonded azodioxide dimer is favored in water. Additionally, nm-size aggregates, displaying sharp NMR signals, form in water. Such an 'NMR-active aggregate' has not been previously reported for a nitrosobenzene. Indeed, we believe the formation of NMR-active aggregates of small organic molecules in water<sup>17</sup> is more common-place than currently realized or reported. The environmental effects on o-NC structure (its degree of DCB) between being dissolved in water and being within the NMR aggregate are dramatic, resulting in shielded signals for the latter (Fig. 3) and a large free energy preference for M in the aggregate but for D in water (Table 1). This further contrasts to the pure Z-dimer form of o-NC in the neat solid state. The NMR-aggregates of o-NC in water are meta-stable, lasting hours in ambient water and having a roughly constant volume/size, suggesting an energy-minimum structure of the nanoaggregate. In D2O, chemical exchange inand-out of the NMR aggregate is observed by EXSY NMR, which also shows M,Dz and M,DE exchanges both inside and outside of the NMR aggregate. Full understanding of NMR-active organic aggregate formation in water and establishment of its generality will provide unprecedented opportunities to perform organic transformations in a sustainable manner.  $^{22,23}\ \mbox{Further}$ study of the assembly processes of o-NC in water as influenced by organic hosts is underway.5

C.H.R., A.P., and L.A.G. performed the experiments, collected, and analyzed the data, with supervision from V.R. and S.C.B. C.H.R., A.P., V.R., and S.C.B. collectively wrote the manuscript. S.A.K. and R.V. performed preliminary studies. Y.L. and P.A.C. performed and analyzed the DFT calculations. K.B. assisted with NMR experiments and L.M.W. performed X-ray crystallography.

V.R. thanks NSF (CHE-2204046) for support. S.C.B and C.H.R acknowledge support by the NSF MRI and The University of Alabama for purchase of an NEO 500 MHz NMR spectrometer (CHE-1919906) and a single-crystal X-ray diffractometer (CHE-1828078). The calculations were performed on the Wulver cluster supported by NJIT.

### Data availability

The data supporting this article have been included in the Supplementary Information.

### **Conflicts of interest**

There are no conflicts to declare.

#### Notes and references

- 1 Y. Jin, C. Yu, R. J. Denman and W. Zhang, *Chem. Soc. Rev.*, 2013, **42**, 6634-6654.
- 2 (a) D. Beaudoin, T. Maris and J. D. Wuest, *Nat. Chem.*, 2013, **5**, 830-834; (b) P. Chakma and D. Konkolewicz, *Angew. Chem. Int. Ed.*, 2019, **58**, 9682-9695; (c) J. Huang, N. Ramlawi, G. S. Sheridan, C. Chen, R. H. Ewoldt, P. V. Braun and C. M. Evans, *Macromolecules*, 2023, **56**, 1253-1262.
- 3 D. Beaudoin and J. D. Wuest, *Chem. Rev.*, 2016, **116**, 258-286.
- 4 H. Vančik, Aromatic C-nitroso compounds, Springer, 2013.

- 5 R. Varadharajan, S. A. Kelley, V. M. Jayasinghe-Arachchige, R. Prabhakar, V. Ramamurthy and S. C. Blackstock, *ACS Org. Inorg. Au*, 2022, **2**, 175-185.
- 6 Biphasic CH<sub>2</sub>Cl<sub>2</sub>/oxone is a generally useful for N-oxygenation reactions (a) S. C. Blackstock, K. Poehling and M. L. Greer, *J. Am. Chem. Soc.*, 1995, 117, 6617-6618; (b) M. L. Greer, B. J. McGee, R. D. Rogers and S. C. Blackstock, *Angew. Chem. Int. Ed. Engl.*, 1997, 36, 1864-1866; (c) B. Priewisch and K. Rück-Braun, *J. Org. Chem.*, 2005, 70, 2350-2352.
- 7 (a) R.-Q. Ran, S.-D. Xiu and C.-Y. Li, *Org. Lett.*, 2014, **16**, 6394-6396; (b) S. A. Kelley, Ph.D. Dissertation, The University of Alabama, 2021.
- 8 D. A. Fletcher, B. G. Gowenlock and K. G. Orrell, *J. Chem. Soc., Perkin Trans.* 2, 1997, 2201-2206.
- 9 DFT calculations (see SI) give a N-phenyl twist barrier of 77.3 kJ/mol (CHCl<sub>3</sub>), consistent with slow rotation at low temperature but fast rotation at ambient on NMR timescale (see S14).
- 10 (a) J. Jeener, B. H. Meier, P. Bachmann and R. R. Ernst, J. Chem. Phys., 1979, 71, 4546-4553; (b) C. L. Perrin and T. J. Dwyer, Chem. Rev., 1990, 90, 935-967.
- 11 K. G. Orrell, V. Šik and D. Stephenson, *Magn. Reson. Chem.*, 1987, **25**, 1007-1011.
- 12 Determined by DFT (ωB97X-D/aug-cc-pVTZ/SMD (CHCl<sub>3</sub>)). See also: K. Varga, I. Biljan, V. K. Varga, I. Biljan, V. Tomišić, Z. Mihalić and H. Vančik, *J. Phys. Chem. A*, 2018, **122**, 2542-2549.
- 13 N. Karschin, S. Krenek, D. Heyer and C. Griesinger, *Magn. Reson. Chem.*, 2022, **60**, 203-209.
- 14 D. A. Fletcher, B. G. Gowenlock and K. G. Orrell, *J. Chem. Soc., Perkin Trans.* 2, 1998, 797-804.
- 15 (a) C. Tanford, *The hydrophobic effect: formation of micelles and biological membranes 2<sup>nd</sup> ed*, John Wiley & Sons, 1980; (b) R. Breslow, in *Organic Reactions in Water: Principles, Strategies and Applications*, Blackwell, 2007, pp. 1-28; (c) S. Narayan, V. V. Fokin and K. B. Sharpless, in *Organic Reactions in Water: Principles, Strategies and Applications*, Blackwell, 2007, pp. 350-365; (d) Y. Jung and R. A. Marcus, *J. Am. Chem. Soc.*, 2007, **129**, 5492-5502.
- 16 o-NC added as a 0.0697 M stock solution in DMSO-d<sub>6</sub>.
- 17 For prior reports of NMR aggregates in water see: (a) D. Carteau, I. Pianet, P. Brunerie, B. Guillemat and D. M. Bassani, *Langmuir*, 2007, **23**, 3561-3565; (b) S. R. LaPlante, R. Carson, J. Gillard, N. Aubry, R. Coulombe, S. Bordeleau, P. Bonneau, M. Little, J. O'Meara and P. L. Beaulieu, *J. Med. Chem.*, 2013, **56**, 5142-5150.
- 18 The  $D_Z$  diastereotopic methyl groups of the 'dissolved' azodioxide in  $D_2O$  show EXSY exchange, indicating conformational interchange by double C.N bond rotations at ambient.
- 19 Figs. S34 and S35 show time domain UV-Vis and DLS data for *o*-NC in water. The DLS data show large 850 nm colloids formed initially at 2.0 mM *o*-NC in water (not observed by NMR), which become more polydisperse with time.
- G. Pagès, V. Gilard, R. Martino and M. Malet-Martino, *Analyst*, 2017, **142**, 3771-3796.
- 21 Calculated using the DOSY radii of M, D, and A, spherical volumes, and the  $M_8D_2$  aggregate stoichiometry
- 22 V. Jeyapalan, R. Varadharajan, G. B. Veerakanellore and V. Ramamurthy, *J. Photochem. Photobiol., A*, 2021, **420**, 113492-113502.
- 23 Y.-M. Tian, W. Silva, R. M. Gschwind and B. König, *Science*, 2024, 383, 750-756.

Page 5 of 5 ChemComm

Data Availability Statement (DAS)

Electronic supplementary information (ESI) available. CCDC 2313924, For EST and crystallographic data in CIF or other electronic formati see <a href="https://www.ccdc.cam.ac.uk/data">www.ccdc.cam.ac.uk/data</a> request/cif DOI: 10.1039/x0xx00000x

ESI file is uploaded checkCIF report is uploaded for crystal structure CCDC